

## An N2HDM Solution for the possible 96 GeV Excess

---

### T. Biekötter

*Instituto de Física Teórica, (UAM/CSIC) &  
Departamento de Física Teórica, Universidad Autónoma de Madrid,  
Cantoblanco, E-28049 Madrid, Spain*  
E-mail: [thomas.biekotter@csic.es](mailto:thomas.biekotter@csic.es)

### M. Chakraborti

*Instituto de Física Teórica, (UAM/CSIC) Universidad Autónoma de Madrid,  
Cantoblanco, E-28049 Madrid, Spain*  
E-mail: [mani.chakraborti@gmail.com](mailto:mani.chakraborti@gmail.com)

### S. Heinemeyer\*

*Instituto de Física Teórica, (UAM/CSIC), Universidad Autónoma de Madrid,  
Cantoblanco, E-28049 Madrid, Spain*  
*Campus of International Excellence UAM+CSIC, Cantoblanco, E-28049, Madrid, Spain*  
*Instituto de Física de Cantabria (CSIC-UC), E-39005 Santander, Spain*  
E-mail: [Sven.Heinemeyer@cern.ch](mailto:Sven.Heinemeyer@cern.ch)

We discuss a  $\sim 3\sigma$  signal (local) in the light Higgs-boson search in the diphoton decay mode at  $\sim 96$  GeV as reported by CMS, together with a  $\sim 2\sigma$  excess (local) in the  $b\bar{b}$  final state at LEP in the same mass range. We review the interpretation of this possible signal as a Higgs boson in the 2 Higgs Doublet Model with an additional real Higgs singlet (N2HDM). It is shown that the lightest Higgs boson of the N2HDM can perfectly fit both excesses simultaneously, while the full Higgs-boson sector is in agreement with all Higgs-boson measurements and exclusion bounds as well as other theoretical and experimental constraints. It is demonstrated that in particular the N2HDM type II and can fit the data best, leading to a supersymmetric interpretation. The NMSSM and the  $\mu\nu$ SJM are briefly reviewed in this respect.

*Corfu Summer Institute 2018 "School and Workshops on Elementary Particle Physics and Gravity"  
(CORFU2018)  
31 August - 28 September, 2018  
Corfu, Greece*

---

\*Speaker.

## 1. Introduction

The Higgs boson discovered in 2012 by ATLAS and CMS [1, 2] – within theoretical and experimental uncertainties – is consistent with the existence of a Standard-Model (SM) Higgs boson [3]. However, the measurements of Higgs-boson couplings, which are known experimentally to a precision of roughly  $\sim 20\%$ , leave room for Beyond Standard-Model (BSM) interpretations. Many BSM models possess extended Higgs-boson sectors, which naturally contain additional Higgs bosons with masses larger than 125 GeV. However, many extensions also offer the possibility of additional Higgs bosons *below* 125 GeV. Consequently, the search for lighter Higgs bosons forms an important part in the BSM Higgs-boson analyses.

Searches for Higgs bosons below 125 GeV have been performed at LEP, the Tevatron and the LHC. LEP reported a  $2.3\sigma$  local excess observed in the  $e^+e^- \rightarrow Z(H \rightarrow b\bar{b})$  searches [4], which would be consistent with a scalar of mass  $\sim 98$  GeV, but due to the  $b\bar{b}$  final state the mass resolution is rather coarse). The excess corresponds to

$$\mu_{\text{LEP}} = \frac{\sigma(e^+e^- \rightarrow Z\phi \rightarrow Zb\bar{b})}{\sigma^{\text{SM}}(e^+e^- \rightarrow ZH \rightarrow Zb\bar{b})} = 0.117 \pm 0.057, \quad (1.1)$$

where the signal strength  $\mu_{\text{LEP}}$  is the measured cross section normalized to the SM expectation, with the SM Higgs-boson mass at  $\sim 98$  GeV. The value for  $\mu_{\text{LEP}}$  was extracted in Ref. [5] using methods described in Ref. [6].

Recent CMS Run II results [7] for Higgs-boson searches in the diphoton final state show a local excess of  $\sim 3\sigma$  around  $\sim 96$  GeV, with a similar excess of  $2\sigma$  in the Run I data at a comparable mass [8]. The excess corresponds to (combining 7, 8 and 13 TeV data, and assuming that the  $gg$  production dominates)

$$\mu_{\text{CMS}} = \frac{\sigma(gg \rightarrow \phi \rightarrow \gamma\gamma)}{\sigma^{\text{SM}}(gg \rightarrow H \rightarrow \gamma\gamma)} = 0.6 \pm 0.2. \quad (1.2)$$

First Run II results from ATLAS with  $80 \text{ fb}^{-1}$  in the  $\gamma\gamma$  searches below 125 GeV turned out to be weaker than the corresponding CMS results, see, e.g., Fig. 1 in Ref. [9].

Reviews about the possibility that these two excesses, found effectively at the same mass, are of a common origin, are given in Refs. [9, 10]. The list comprises of type I 2HDMs [11, 12], a radion model [13], a minimal dilaton model [14], as well as supersymmetric models [15–17].

Motivated by the Hierarchy Problem, Supersymmetry (SUSY) plays a prominent role in BSM physics. The simplest SUSY extension of the SM is the Minimal Supersymmetric Standard Model (MSSM) [18, 19], doubling the degrees of freedom of the SM supplemented with a second Higgs doublet. The MSSM Higgs sector, composed of  $\Phi_1$  and  $\Phi_2$ , consists of two  $\mathcal{C}\mathcal{P}$ -even, one  $\mathcal{C}\mathcal{P}$ -odd and two charged Higgs bosons. The light (or the heavy)  $\mathcal{C}\mathcal{P}$ -even MSSM Higgs boson can be interpreted as the signal discovered at  $\sim 125$  GeV [20] (see Refs. [21, 22] for recent updates). However, in Ref. [21] it was demonstrated that the MSSM cannot explain the CMS excess in the diphoton final state. This can be traced back to the “too rigid” structure of the 2HDM (type II) structure of the Higgs-boson sector in the MSSM.

This raises the question whether simple extensions of the 2HDM can fit both the CMS excess in Eq. (1.2) and the LEP excesses in Eq. (1.1). In Ref. [23] the Next to minimal 2 Higgs doublet

model (N2HDM) [24, 25] was investigated. In this model the two Higgs doublets are supplemented with a real Higgs singlet, giving rise to one additional (potentially light)  $\mathcal{C}\mathcal{P}$ -even Higgs boson. However, in comparison to SUSY models the N2HDM does not have to obey the SUSY relations in the Higgs-boson sector. Consequently, it allows to study how the potential fits the two excesses simultaneously in a more general way. Here we review first the results obtained in the N2HDM [23] and then two possible SUSY realizations.

## 2. The N2HDM, constraints and the experimental excesses

### 2.1 The N2HDM

The N2HDM is the simplest extension of a  $\mathcal{C}\mathcal{P}$ -conserving two Higgs doublet model (2HDM) in which the latter is augmented with a real scalar singlet Higgs field, denoted as  $\Phi_1$ ,  $\Phi_2$  and  $\Phi_S$ , respectively (see, e.g., Refs. [24, 25]). As in the 2HDM a  $Z_2$  symmetry is imposed to avoid flavor changing neutral currents at the tree-level, only softly broken in the Higgs sector via the bilinear mass term  $m_{12}^2(\Phi_1^\dagger\Phi_2 + h.c.)$ . As in the 2HDM, this leads to four variants of the N2HDM, depending on the  $Z_2$  parities of the fermions. Taking the electroweak symmetry breaking (EWSB) minima to be charge and  $\mathcal{C}\mathcal{P}$ -conserving, the scalar fields after EWSB can be parametrised as

$$\Phi_1 = \begin{pmatrix} \phi_1^+ \\ \frac{1}{\sqrt{2}}(v_1 + \rho_1 + i\eta_1) \end{pmatrix}, \quad \Phi_2 = \begin{pmatrix} \phi_2^+ \\ \frac{1}{\sqrt{2}}(v_2 + \rho_2 + i\eta_2) \end{pmatrix}, \quad \Phi_S = v_S + \rho_S, \quad (2.1)$$

where  $v_1, v_2, v_S$  are the real vevs acquired by the fields  $\Phi_1, \Phi_2$  and  $\Phi_S$  respectively. As in the 2HDM we define  $\tan\beta := v_2/v_1$ . The  $\mathcal{C}\mathcal{P}$ -even Higgs-boson sector contains three physical Higgses. Thus, a rotation from the interaction to the physical basis can be achieved with the help of a  $3 \times 3$  orthogonal matrix as

$$\begin{pmatrix} h_1 \\ h_2 \\ h_3 \end{pmatrix} = R \begin{pmatrix} \rho_1 \\ \rho_2 \\ \rho_S \end{pmatrix}, \quad (2.2)$$

with  $m_{h_1} < m_{h_2} < m_{h_3}$ . The rotation matrix  $R$  can be parametrized as

$$R = \begin{pmatrix} c_{\alpha_1}c_{\alpha_2} & s_{\alpha_1}c_{\alpha_2} & s_{\alpha_2} \\ -(c_{\alpha_1}s_{\alpha_2}s_{\alpha_3} + s_{\alpha_1}c_{\alpha_3}) & c_{\alpha_1}c_{\alpha_3} - s_{\alpha_1}s_{\alpha_2}s_{\alpha_3} & c_{\alpha_2}s_{\alpha_3} \\ -c_{\alpha_1}s_{\alpha_2}c_{\alpha_3} + s_{\alpha_1}s_{\alpha_3} & -(c_{\alpha_1}s_{\alpha_3} + s_{\alpha_1}s_{\alpha_2}c_{\alpha_3}) & c_{\alpha_2}c_{\alpha_3} \end{pmatrix}, \quad (2.3)$$

$\alpha_1, \alpha_2, \alpha_3$  being the three mixing angles, and we use the short-hand notation  $s_x = \sin x$ ,  $c_x = \cos x$ . The couplings of the Higgs bosons to SM particles are modified w.r.t. the SM Higgs-coupling predictions due to the mixing in the Higgs sector. It is convenient to express the couplings of the scalar mass eigenstates  $h_i$  normalized to the corresponding SM couplings. We therefore introduce the coupling coefficients  $c_{h_iVV}$  and  $c_{h_i f\bar{f}}$ , such that the couplings to the massive vector bosons are given by

$$(g_{h_i WW})_{\mu\nu} = ig_{\mu\nu}(c_{h_iVV})gM_W \quad \text{and} \quad (g_{h_i ZZ})_{\mu\nu} = ig_{\mu\nu}(c_{h_iVV})\frac{gM_Z}{c_w}, \quad (2.4)$$

	$u$ -type ( $c_{h_i t \bar{t}}$ )	$d$ -type ( $c_{h_i b \bar{b}}$ )	leptons ( $c_{h_i \tau \bar{\tau}}$ )
type I	$R_{i2}/s_\beta$	$R_{i2}/s_\beta$	$R_{i2}/s_\beta$
type II	$R_{i2}/s_\beta$	$R_{i1}/c_\beta$	$R_{i1}/c_\beta$
type III (lepton-specific)	$R_{i2}/s_\beta$	$R_{i2}/s_\beta$	$R_{i1}/c_\beta$
type IV (flipped)	$R_{i2}/s_\beta$	$R_{i1}/c_\beta$	$R_{i2}/s_\beta$

**Table 1:** Coupling factors of the Yukawa couplings of the N2HDM Higgs bosons  $h_i$  w.r.t. their SM values.

where  $g$  is the  $SU(2)_L$  gauge coupling,  $c_w$  the cosine of weak mixing angle,  $c_w = M_W/M_Z$ ,  $s_w = \sqrt{1 - c_w^2}$ , and  $M_W$  and  $M_Z$  the masses of the  $W$  boson and the  $Z$  boson, respectively. The couplings of the Higgs bosons to the SM fermions are given by

$$g_{h_i f \bar{f}} = \frac{m_f}{v} (c_{h_i f \bar{f}}), \quad (2.5)$$

where  $m_f$  is the mass of the fermion and  $v = \sqrt{(v_1^2 + v_2^2)}$  is the SM vev. The coupling coefficients for the couplings to gauge bosons  $V = W, Z$  for the three  $\mathcal{C}\mathcal{P}$ -even Higgses. are identical in all four types of the (N)2HDM. They differ, however, as in the 2HDM depending on the type of the model, as summarized in Tab. 1.

There are 12 independent parameters in the model, which can be taken as [25];

$$\alpha_{1,2,3}, \quad \tan\beta, \quad v, \quad v_S, \quad m_{h_{1,2,3}}, \quad m_A, \quad M_{H^\pm}, \quad m_{12}^2, \quad (2.6)$$

where  $m_A, M_{H^\pm}$  denote the masses of the physical  $\mathcal{C}\mathcal{P}$ -odd and charged Higgses respectively.

In Ref. [23] the code `ScannerS` [25, 26] has been used to uniformly explore the set of independent parameters as given in Eq. (2.6) (see below). The lightest  $\mathcal{C}\mathcal{P}$ -even Higgs boson,  $h_1$ , was identified with the one being potentially responsible for the signal at  $\sim 96$  GeV. The second lightest  $\mathcal{C}\mathcal{P}$ -even Higgs boson was identified with the one observed at  $\sim 125$  GeV.

## 2.2 Constraints

All relevant constraints on the N2HDM were taken into account, see Ref. [23] for more details. These comprise

- Theoretical constraints:  
tree-level perturbativity and the condition that the vacuum should be a global minimum of the potential.
- Constraints from direct searches at colliders:  
All relevant searches for BSM Higgs bosons are taken into account with the code `HiggsBounds v. 5.3.2` [27–31].
- Constraints from the SM-like Higgs-boson properties:  
Any model beyond the SM has to accommodate the SM-like Higgs boson, with mass and signal strengths as they were measured at the LHC. In our scans the compatibility of the  $\mathcal{C}\mathcal{P}$ -even scalar  $h_2$  with a mass of 125.09 GeV with the measurements of signal strengths at Tevatron and LHC is checked with the code `HiggsSignals v. 2.2.3` [32–34]. The

corresponding theory predictions are proved by a combination of the codes `ScannerS`, `SuSHi` [35, 36] and `N2HDECAY` [25, 37, 38]. The `HiggsSignals` output shown below consists in the reduced  $\chi^2$ ,

$$\chi_{\text{red}}^2 = \frac{\chi^2}{n_{\text{obs}}}, \quad (2.7)$$

where  $\chi^2$  is provided by `HiggsSignals` and  $n_{\text{obs}} = 101$  is the number of experimental observations considered.

- Constraints from flavor physics:

In the low  $\tan\beta$  region that is of interest (see below) the constraints which must be taken into account are [39]:  $\text{BR}(B \rightarrow X_s \gamma)$ , constraints on  $\Delta M_{B_s}$  from neutral  $B$ -meson mixing and  $\text{BR}(B_s \rightarrow \mu^+ \mu^-)$ . Constraints from  $\text{BR}(B \rightarrow X_s \gamma)$  excludes  $M_{H^\pm} < 650$  GeV for all values of  $\tan\beta \gtrsim 1$  in the type II and IV 2HDM, while for type I and III the bounds are more  $\tan\beta$ -dependent.

- Constraints from electroweak precision data:

Constraints from electroweak precision observables can in a simple approximation be expressed in terms of the oblique parameters  $S$ ,  $T$  and  $U$  [40, 41]. Deviations to these parameters are significant if new physics beyond the SM enters mainly through gauge boson self-energies, as it is the case for extended Higgs sectors. These constraints are implemented in `ScannerS`. For points to be in agreement with the experimental observation, it was required that the prediction of the  $S$  and the  $T$  parameter are within the  $2\sigma$  ellipse, corresponding to  $\chi^2 = 5.99$  for two degrees of freedom.

### 2.3 Experimental excesses

As experimental input for the signal strengths in Ref. [23] the values

$$\mu_{\text{LEP}} = 0.117 \pm 0.057 \quad \text{and} \quad \mu_{\text{CMS}} = 0.6 \pm 0.2 \quad (2.8)$$

were used, as quoted in Refs. [5, 42] and [7, 43].

The evaluation of the signal strengths for the excesses was done in the narrow width approximation. For the LEP excess this is given by,

$$\mu_{\text{LEP}} = \frac{\sigma_{\text{N2HDM}}(e^+e^- \rightarrow Zh_1)}{\sigma_{\text{SM}}(e^+e^- \rightarrow ZH)} \cdot \frac{\text{BR}_{\text{N2HDM}}(h_1 \rightarrow b\bar{b})}{\text{BR}_{\text{SM}}(H \rightarrow b\bar{b})} = |c_{h_1VV}|^2 \frac{\text{BR}_{\text{N2HDM}}(h_1 \rightarrow b\bar{b})}{\text{BR}_{\text{SM}}(H \rightarrow b\bar{b})}, \quad (2.9)$$

evaluated with the help of `N2HDECAY`. For the CMS signal strength one finds,

$$\mu_{\text{CMS}} = \frac{\sigma_{\text{N2HDM}}(gg \rightarrow h_1)}{\sigma_{\text{SM}}(gg \rightarrow H)} \cdot \frac{\text{BR}_{\text{N2HDM}}(h_1 \rightarrow \gamma\gamma)}{\text{BR}_{\text{SM}}(H \rightarrow \gamma\gamma)} = |c_{h_1\tilde{t}\tilde{t}}|^2 \frac{\text{BR}_{\text{N2HDM}}(h_1 \rightarrow \gamma\gamma)}{\text{BR}_{\text{SM}}(H \rightarrow \gamma\gamma)}. \quad (2.10)$$

The SM predictions for the branching ratios and the cross section via ggF can be found in Ref. [44].

As can be seen from Eqs. (2.8) - (2.10), the CMS excess points towards the existence of a scalar with a SM-like production rate, whereas the LEP excess demands that the scalar should have a squared coupling to massive vector bosons of  $\sim 0.1$  times that of the SM Higgs boson of the same mass. This suppression of the coupling coefficient  $c_{h_1VV}$  is naturally fulfilled for a singlet-like

	Decrease $c_{h_1 b\bar{b}}$	No decrease $c_{h_1 t\bar{t}}$	No enhancement $c_{h_1 \tau\bar{\tau}}$
type I	✓ ( $\frac{R_{12}}{s_\beta}$ )	✗ ( $\frac{R_{12}}{s_\beta}$ )	✓ ( $\frac{R_{12}}{s_\beta}$ )
type II	✓ ( $\frac{R_{11}}{c_\beta}$ )	✓ ( $\frac{R_{12}}{s_\beta}$ )	✓ ( $\frac{R_{11}}{c_\beta}$ )
lepton-specific	✓ ( $\frac{R_{12}}{s_\beta}$ )	✗ ( $\frac{R_{12}}{s_\beta}$ )	✗ ( $\frac{R_{11}}{c_\beta}$ )
flipped	✓ ( $\frac{R_{11}}{c_\beta}$ )	✓ ( $\frac{R_{12}}{s_\beta}$ )	✗ ( $\frac{R_{12}}{s_\beta}$ )

**Table 2:** Conditions that have to be satisfied to accommodate the LEP and CMS excesses simultaneously with a light  $\mathcal{C}\mathcal{P}$ -even scalar  $h_1$  with dominant singlet component. In brackets we state the relevant coupling coefficients  $c_{h_1 f\bar{f}}$  for the conditions for each type.

state, that acquires its interaction to SM particles via a considerable mixing with the SM-like Higgs boson, thus motivating the explanation of the LEP excess with the real singlet of the N2HDM. For the CMS excess, on the other hand, it appears to be difficult at first sight to accommodate the large signal strength, because one expects a suppression of the loop-induced coupling to photons of the same order as the one of  $c_{h_1 VV}$ , since in the SM the Higgs-boson decay to photons is dominated by the  $W$  boson loop. However, it turns out that it is possible to overcompensate the suppression of the loop-induced coupling to photons by decreasing the total width of the singlet-like scalar, leading to an enhancement of the branching ratio of the new scalar to the  $\gamma\gamma$  final state. The different types of N2HDM behave differently in this regard, based on how the doublet fields are coupled to the quarks and leptons. The general idea is summarized in Tab. 2.

In Ref. [23] it was argued that only the type II and type IV (flipped) N2HDM can accommodate both excesses simultaneously using a dominantly singlet-like scalar  $h_1$  at  $\sim 96$  GeV. The first condition is that the coupling of  $h_1$  to  $b$ -quarks has to be suppressed to enhance the decay rate to  $\gamma\gamma$ , as the total decay width at this mass is still dominated by the decay to  $b\bar{b}$ . At the same time one can not decrease the coupling to  $t$ -quarks too much, because the decay width to photons strongly depends on the top quark loop contribution (interfering constructively with the charged Higgs contribution). Moreover, the ggF production cross section is dominated at leading order by the diagram with  $t$ -quarks in the loop. Thus, a decreased coupling of  $h_1$  to  $t$ -quarks implies a lower production cross section at the LHC. As one can deduce from Tab. 2, in type I and type III of the N2HDM, the coupling coefficients are the same for up- and down-type quarks. Thus, it is impossible to satisfy both of the above criteria simultaneously in these models. Consequently, they fail to accommodate both the CMS and the LEP excesses and are discarded from now on.

In Ref. [23] it is furthermore concluded that in type II and IV that  $|\alpha_1| \rightarrow \pi/2$  corresponds to an enhancement of the branching ratio to photons, because the dominant decay width to  $b$ -quarks, and therefore the total width of  $h_1$ , is suppressed.

A third condition, although not as significant as the other two, is related to the coupling of  $h_1$  to leptons. If it is increased, the decay to a pair of  $\tau$ -leptons will be enhanced. Similar to the decay to  $b$ -quarks, it will compete with the diphoton decay and can suppress the signal strength needed for the CMS excess. The  $\tau$ -Yukawa coupling is not as large as the  $b$ -Yukawa coupling, so this condition is not as important as the other two. Still, as will be reviewed below, it is the reason why it is easier to fit the CMS excess in the type II model compared to the flipped scenario.

In the scans we indicate the “best-fit point” referring to the point with the smallest  $\chi^2$  defined

by

$$\chi_{\text{CMS-LEP}}^2 = \frac{(\mu_{\text{LEP}} - 0.117)^2}{0.057^2} + \frac{(\mu_{\text{CMS}} - 0.6)^2}{0.2^2}, \quad (2.11)$$

quantifying the quadratic deviation w.r.t. the measured values, assuming that there is no correlation between the signal strengths of the two excesses.

### 3. Results

In the following we will describe the analysis in the type II (with similar results in type IV [23]). The scalar mass eigenstate with dominant singlet-component will be responsible for accommodating the LEP and the CMS excesses at  $\sim 95$ -98 GeV. The second lightest Higgs-boson will be placed at  $\sim 125$  GeV with the requirement that it behaves within the uncertainties as the SM Higgs-boson. Similar scans have been performed also for the N2HDM type I and III (lepton specific), confirming that these types cannot fit well the two excesses.

The following ranges of input parameters have been scanned:

$$\begin{aligned} 95 \text{ GeV} \leq m_{h_1} \leq 98 \text{ GeV}, \quad m_{h_2} = 125.09 \text{ GeV}, \quad 400 \text{ GeV} \leq m_{h_3} \leq 1000 \text{ GeV}, \\ 400 \text{ GeV} \leq m_A \leq 1000 \text{ GeV}, \quad 650 \text{ GeV} \leq M_{H^\pm} \leq 1000 \text{ GeV}, \\ 0.5 \leq \tan \beta \leq 4, \quad 0 \leq m_{12}^2 \leq 10^6 \text{ GeV}^2, \quad 100 \text{ GeV} \leq v_S \leq 1500 \text{ GeV}. \end{aligned} \quad (3.1)$$

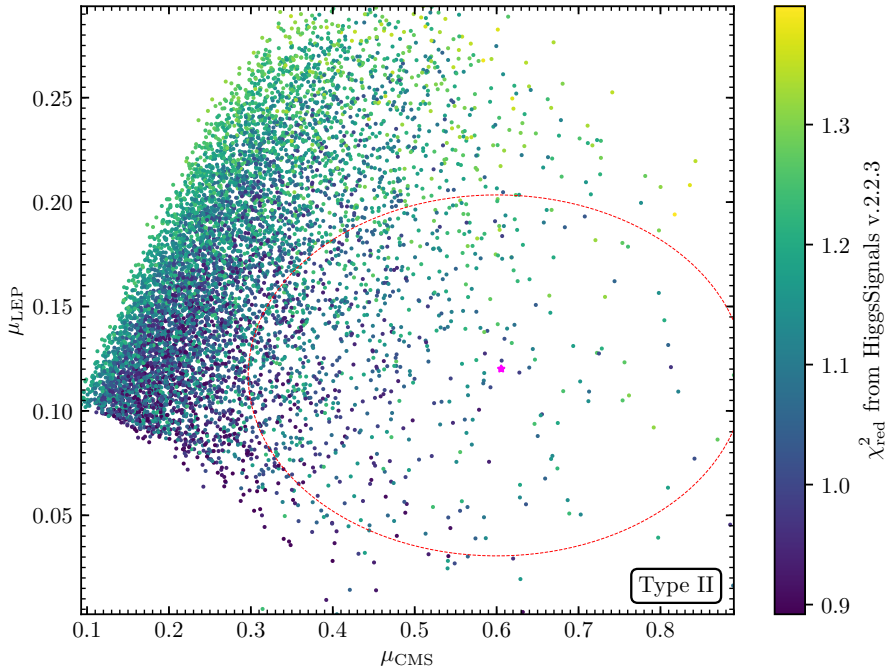


**Figure 1:** Type II: the signal strengths  $\mu_{\text{CMS}}$  and  $\mu_{\text{LEP}}$  are shown for each scan point respecting the experimental and theoretical constrains. The  $1\sigma$ -region of both excesses is shown by the red ellipse. The colors show the the  $\chi_{\text{red}}^2$  from HiggsSignals. The best-fit point (magenta) has  $\chi_{\text{red}}^2 = 1.237$  with 101 observations considered. The lowest (highest) value of  $\chi_{\text{red}}^2$  inside the  $1\sigma$  ellipse is 0.9052 (1.3304).

$m_{h_1}$	$m_{h_2}$	$m_{h_3}$	$m_A$	$M_{H^\pm}$		
96.5263	125.09	535.86	712.578	737.829		
$\tan\beta$	$\alpha_1$	$\alpha_2$	$\alpha_3$	$m_{12}^2$	$v_S$	
1.26287	1.26878	-1.08484	-1.24108	80644.3	272.72	
$\text{BR}_{h_1}^{bb}$	$\text{BR}_{h_1}^{gg}$	$\text{BR}_{h_1}^{cc}$	$\text{BR}_{h_1}^{\tau\tau}$	$\text{BR}_{h_1}^{\gamma\gamma}$	$\text{BR}_{h_1}^{WW}$	$\text{BR}_{h_1}^{ZZ}$
0.5048	0.2682	0.1577	0.0509	$2.582 \cdot 10^{-3}$	0.0137	$1.753 \cdot 10^{-3}$
$\text{BR}_{h_2}^{bb}$	$\text{BR}_{h_2}^{gg}$	$\text{BR}_{h_2}^{cc}$	$\text{BR}_{h_2}^{\tau\tau}$	$\text{BR}_{h_2}^{\gamma\gamma}$	$\text{BR}_{h_2}^{WW}$	$\text{BR}_{h_2}^{ZZ}$
0.5916	0.0771	0.0288	0.0636	$2.153 \cdot 10^{-3}$	0.2087	0.0261
$\text{BR}_{h_3}^{tt}$	$\text{BR}_{h_3}^{gg}$	$\text{BR}_{h_3}^{h_1 h_1}$	$\text{BR}_{h_3}^{h_1 h_2}$	$\text{BR}_{h_3}^{h_2 h_2}$	$\text{BR}_{h_3}^{WW}$	$\text{BR}_{h_3}^{ZZ}$
0.8788	$2.537 \cdot 10^{-3}$	0.0241	0.0510	$3.181 \cdot 10^{-3}$	0.0261	0.0125
$\text{BR}_A^{tt}$	$\text{BR}_A^{gg}$	$\text{BR}_A^{Zh_1}$	$\text{BR}_A^{Zh_3}$	$\text{BR}_A^{bb}$		
0.6987	$1.771 \cdot 10^{-3}$	0.1008	0.1981	$5.36 \cdot 10^{-4}$		

**Table 3:** Parameters of the best-fit point and branching ratios of the lightest, second lightest and heavy  $\mathcal{C}\mathcal{P}$ -even scalar and the  $\mathcal{C}\mathcal{P}$ -odd scalar in the type II scenario. Dimensionful parameters are given in GeV and the angles are given in radian.

We show the result of the scan in Fig. 1 [23] in the plane of the signal strengths  $\mu_{\text{LEP}}$  and  $\mu_{\text{CMS}}$  for each scan point, where the best-fit point w.r.t. the two excesses is marked by a magenta star. It should be kept in mind that the density of points has no physical meaning and is a pure artefact of the “flat prior” in our parameter scan. The red dashed line corresponds to the  $1\sigma$  ellipse, i.e., to  $\chi_{\text{CMS-LEP}}^2 = 2.30$  for two degrees of freedom, with  $\chi_{\text{CMS-LEP}}^2$  defined in Eq. (2.11). The colors of the points indicate the reduced  $\chi^2$  from the test of the SM-like Higgs-boson properties with `HiggsSignals`. One sees that various points fit both excesses simultaneously while also accommodating the properties of the SM-like Higgs boson at 125 GeV. The lowest (highest) value of  $M_{H^\pm}$  in the  $1\sigma$  ellipse is 650.03(964.71) GeV, whereas the the lowest (highest) value of  $\tan\beta$  is found to be 0.797 (3.748). It should be emphasized that the dependence of the branching ratio of  $h_1$  to diphotons, and therefore of  $\mu_{\text{CMS}}$ , on  $M_{H^\pm}$  is due to the positive correlation between  $M_{H^\pm}$  and the total decay width of  $h_1$ . The additional contributions to the diphoton decay width of diagrams with the charged Higgs boson in the loop has a minor dependence on  $M_{H^\pm}$  for  $M_{H^\pm} > 650$  GeV.

In Tab. 3 we review the values of the free parameters and the relevant branching ratios of the neutral scalars for the best-fit point of our scan, which is highlighted with a magenta star in Figs. 1. Remarkably, the branching ratio for the singlet-like scalar to photons is larger than the one of the SM-like Higgs boson. As explained in the beginning of Sect. 3 this is achieved by a value of  $\alpha_1 \sim \pi/2$ , which suppresses the decay to  $b$ -quarks and  $\tau$ -leptons, without decreasing the coupling to  $t$ -quarks. Constraints from the oblique parameters lead to a  $\mathcal{C}\mathcal{P}$ -odd Higgs-boson mass  $m_A$  or a heavy  $\mathcal{C}\mathcal{P}$ -even Higgs-boson mass  $m_{h_3}$  close to the mass of the charged Higgs boson.

## 4. Future searches

### 4.1 Indirect searches

Currently, uncertainties on the measurement of the coupling strengths of the SM-like Higgs boson at the LHC are still large, i.e., at the  $1\sigma$ -level they are of the same order as the modifications of the couplings present in our analysis in the N2HDM [3, 47, 48]. In the future, once the complete  $300\text{fb}^{-1}$  collected at the LHC are analyzed, the constraints on the couplings of the SM-like Higgs boson will benefit from the reduction of statistical uncertainties. Even tighter constraints are expected from the LHC after the high-luminosity upgrade (HL-LHC), when the planned amount of  $3000\text{fb}^{-1}$  integrated luminosity will have been collected [49]. Finally, a future linear  $e^+e^-$  collider like the ILC, CLIC, FCC-ee or CepC could improve the precision measurements of the Higgs-boson couplings even further [49, 50], where we will use ILC numbers for illustration. At an  $e^+e^-$  collider the cross section of the Higgs boson can be measured independently, and the total width (and therefore also the coupling modifiers) can be reconstructed without model assumptions.

Several studies have been performed to estimate the future constraints on the coupling modifiers of the SM-like Higgs boson at the LHC [49, 51–54] and the ILC [45, 46, 49, 55–58], assuming that no deviations from the SM predictions will be found. Here, we review the comparison of the scan points to the expected precisions of the HL-LHC and the ILC as they are reported in Refs. [45, 46], neglecting possible correlations of the coupling modifiers. The results are shown in Fig. 2 [23].

We plot the effective coupling coefficient of the SM-like Higgs boson  $h_2$  to  $\tau$ -leptons on the horizontal axis against the coupling coefficient to  $b$ -quarks (top) and to  $t$ -quarks (bottom) for both types. These points passed all the experimental and theoretical constraints, including the verification of SM-like Higgs-boson properties in agreement with LHC results using `HiggsSignals`. In the top plot the blue points lie on a diagonal line, because in type II the coupling to leptons and to down-type quarks scale identically, while in the bottom plot the red points representing the type IV scenario lie on the diagonal, because there the lepton-coupling scales in the same way as the coupling to up-type quarks.

In Fig. 2 the current measurements on the coupling modifiers by ATLAS [48] and CMS [47] are shown as black ellipses. The magenta ellipse in each plot shows the expected precision of the measurement of the coupling coefficients at the  $1\sigma$ -level at the HL-LHC from Ref. [45]. The current uncertainties and the HL-LHC analysis are based on the coupling modifier, or  $\kappa$ -framework, in which the tree-level couplings of the SM-like Higgs boson to vector bosons, the top quark, the bottom quark, the  $\tau$  and the  $\mu$  lepton, and the three loop-induced couplings to  $\gamma\gamma$ ,  $gg$  and  $Z\gamma$  receive a factor  $\kappa_i$  quantifying potential modifications from the SM predictions. These modifiers are then constrained using a global fit to projected HL-LHC data assuming no deviation from the SM prediction will be found. The uncertainties found for the  $\kappa_i$  can directly be applied to the future precision of the coupling modifiers  $c_{h_i,\dots}$  we use in our paper. We use the uncertainties given under the assumptions that no decay of the SM-like Higgs boson to BSM particles is present, and that current systematic uncertainties will be reduced in addition to the reduction of statistical uncertainties due to the increased statistics.

The green and the orange ellipses show the corresponding expected uncertainties when the HL-LHC results are combined with projected data from the ILC after the 250 GeV phase and the

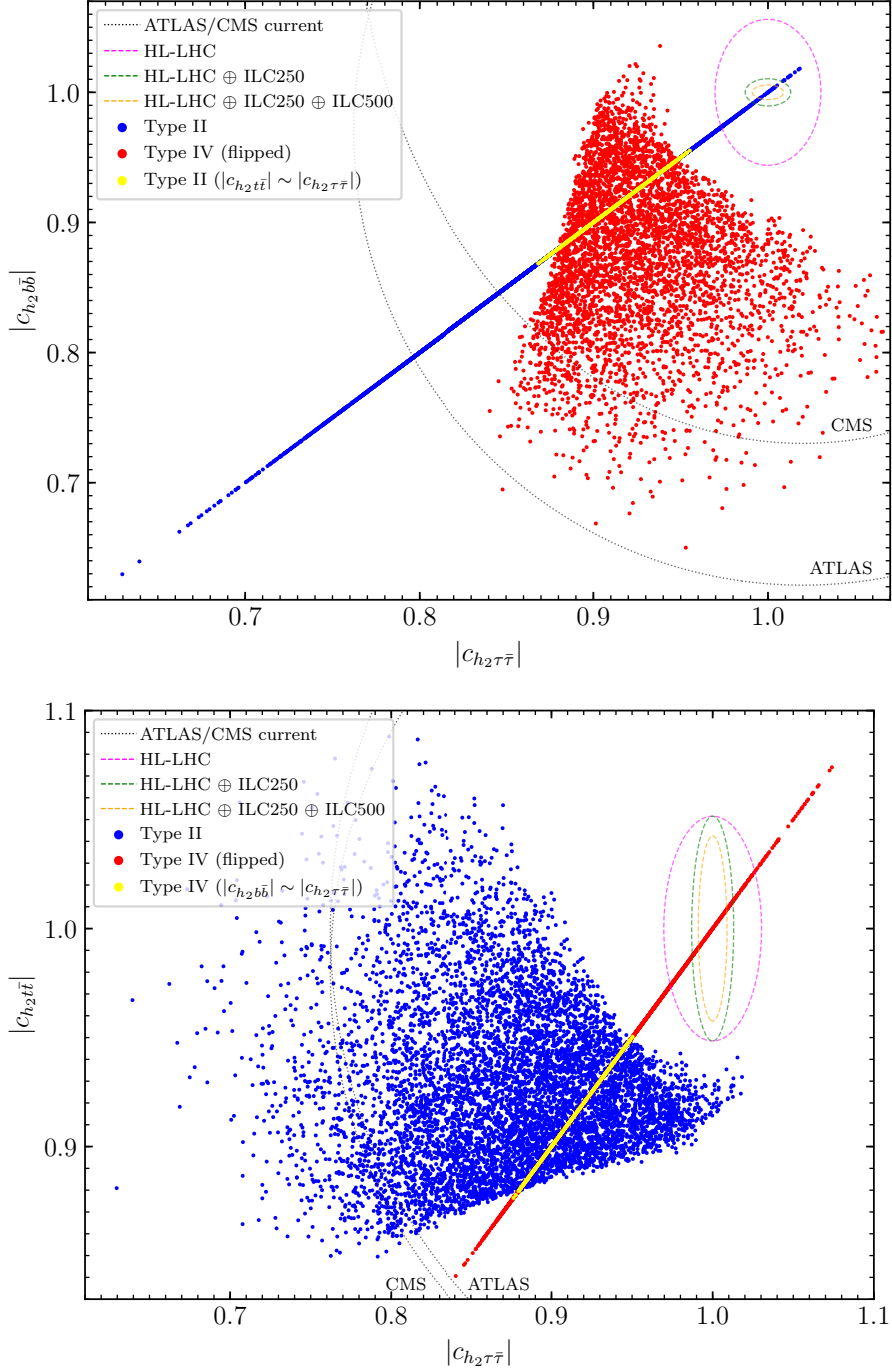


**Figure 2:** Scan points of the analysis in the type II (blue) and type IV (red) scenario in the  $|c_{h_2 \tau \tau}|$ - $|c_{h_2 b \bar{b}}|$  plane (top) and the  $|c_{h_2 \tau \tau}|$ - $|c_{h_2 t \bar{t}}|$  plane (bottom). In the upper plot we highlight in yellow the points of the type II scenario that overlap with points from the type IV scenario in the lower plot, i.e., points with  $|c_{h_2 t \bar{t}}| \sim |c_{h_2 b \bar{b}}| \sim |c_{h_2 \tau \tau}|$ . In the same way in the lower plot we highlight in yellow the points of the type IV scenario that overlap with points from the type II scenario in the upper plot. The dashed ellipses are the projected uncertainties at the HL-LHC [45] (magenta) and the ILC [46] (green and orange) of the measurements of the coupling modifiers at the 68% confidence level, assuming that no deviation from the SM prediction will be found (more details in the text). We also show with the dotted black lines the  $1\sigma$  ellipses of the current measurements from CMS [47] and ATLAS [48].

500 GeV phase, respectively, taken from Ref. [46]. Their analysis is based on a pure effective field theory calculation, supplemented by further assumptions to facilitate the combination with the HL-LHC projections in the  $\kappa$ -framework. In particular, in the effective field theory approach the vector boson couplings can be modified beyond a simple rescaling. This possibility was excluded by recasting the fit setting two parameters related to the couplings to the Z-boson and the W-boson to zero (for details we refer to Ref. [46]).

Remarkably, the expected constraints from the HL-LHC and the ILC will strongly reduce the allowed parameter spaces and allow a clear test of the models under consideration. Independent of the type of the N2HDM, we can see comparing both plots in Fig. 2, that there is not a single scan point that coincides with the SM prediction regarding the three coupling coefficients shown. This implies that, once these couplings are measured precisely by the HL-LHC and the ILC, a deviation of the SM prediction has to be measured in at least one of the couplings, if our explanation of the excesses is correct. Accordingly, if no deviation from the SM prediction regarding these couplings will be measured, our explanation would be ruled out entirely.

Furthermore, in case a deviation from the SM prediction will be found, the predicted scaling behavior of the coupling coefficients in the type II scenario (upper plot) and the type IV scenario (lower plot), might lead to distinct possibilities for the two models to accommodate these possible deviations. In this case, precision measurements of the SM-like Higgs boson couplings could be used to exclude one of the two scenarios. This is true for all points except the ones highlighted in yellow in Fig. 2. The yellow points are a subset of points of our scans that, if such deviations of the SM-like Higgs boson couplings will be measured, could correspond to a benchmark point of both the scan in the type II and the type IV scenario. However, note that this subset of points is confined to the diagonal lines of both plots, and thus corresponds to a very specific subset of the overall allowed parameter space. For the type II scenario, in the upper plot, the yellow points are determined by the additional constraint that  $|c_{h_2 t \bar{t}}| \sim |c_{h_2 \tau \bar{\tau}}|$ , which is exactly true in the type IV scenario. For the type IV scenario, in the lower plot, the yellow points are determined by the additional constraint that  $|c_{h_2 b \bar{b}}| \sim |c_{h_2 \tau \bar{\tau}}|$ , which is exactly true in the type II scenario.

For completeness we show in Fig. 3 the absolute value of the coupling modifier of the SM-like Higgs boson w.r.t. the vector boson couplings  $|c_{h_2 VV}|$  on the vertical axis. Again, the parameter points of both types show deviations larger than the projected experimental uncertainty at HL-LHC and ILC. The deviations in  $|c_{h_2 VV}|$  are even stronger than for the couplings to fermions. A  $2\sigma$  deviation from the SM prediction is expected with HL-LHC accuracy. At the ILC a deviation of more than  $5\sigma$  would be visible. As mentioned already, a suppression of the coupling to vector bosons is explicitly expected by demanding  $\Sigma_{h_2} \geq 10\%$ . However, since points with lower singlet component cannot accommodate both excesses, this does not contradict the conclusion that the explanation of both excesses can be probed with high significance with future Higgs-boson coupling measurements.

## 4.2 Direct searches

To start with, the diphoton bump which has persisted through LHC Run I and II is worth exploring in additional Higgs boson searches of future runs of the LHC. Furthermore, the search for charged Higgs bosons appears promising in the region of low  $\tan\beta$ . Searches at the (HL-)LHC will yield strong constraints or (hopefully) discover signs of a charged Higgs-boson in the region

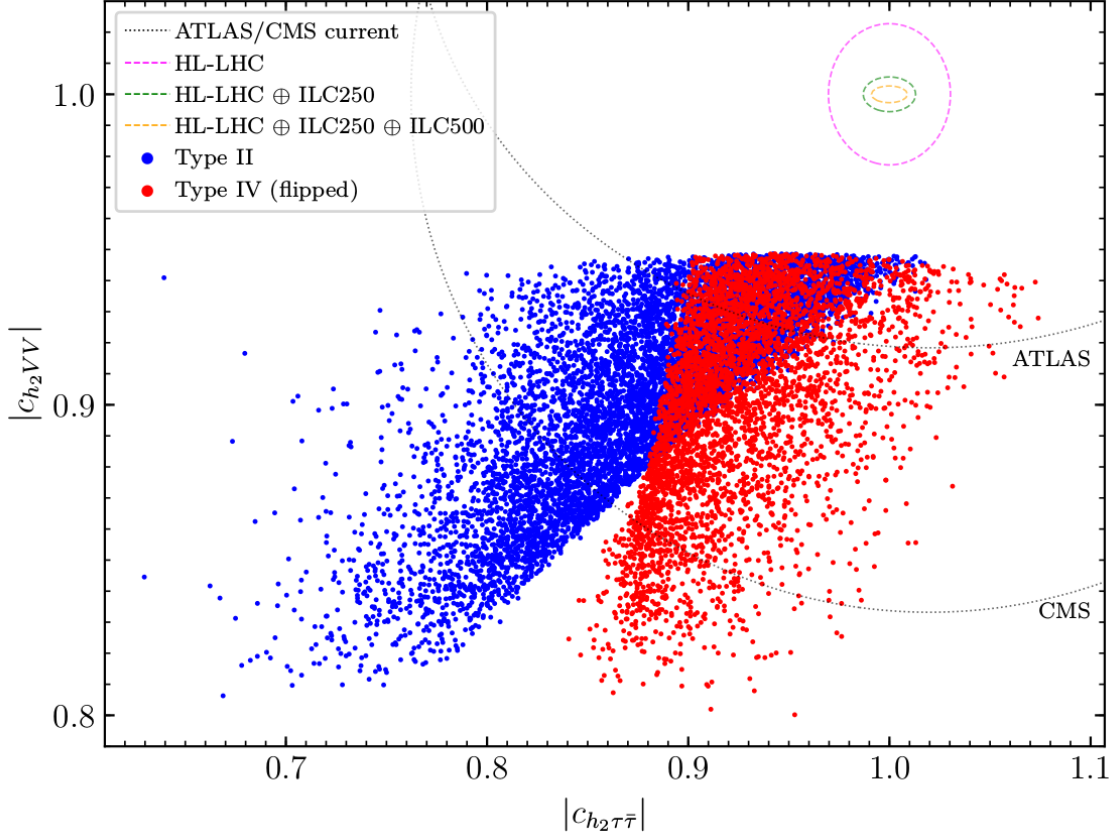


**Figure 3:** As in Fig. 2 but with  $|c_{h_2 V V}|$  on the vertical axis.

between 600 GeV and 950 GeV. Prospects for a  $5\sigma$  discovery in the charged Higgs-boson searches in the  $tb$  decay mode can be found in Ref. [59].

Since the charged Higgs boson is rather heavy due to the constraints from flavor physics, exotic signals at colliders can be expected from the decay of the charged Higgs boson into a  $W$  boson and a neutral Higgs bosons. We show the corresponding branching ratios in Fig. 4, 5 and 6 for the decays of  $H^\pm$  into  $W^\pm$  and  $h_1$ ,  $h_2$  and  $h_3$ , respectively. The blue points are the ones that lie inside the  $1\sigma$  ellipse of  $\mu_{LEP}$  and  $\mu_{CMS}$ . The decays into the two light Higgs bosons is always kinematically allowed. However, as one can see in Fig. 6, if the decay to the heavy Higgs boson  $h_3$  opens up kinematically, it is usually the dominant of the three, and competes with ordinary decay modes of  $H^\pm$  into a pair of  $tb$  quarks. The smallest branching ratio for the mass range of  $M_{H^\pm}$  in our scan is the one to the SM-like Higgs boson  $h_2$ , which is minimized in the limit of  $h_2$  becoming SM-like. Concerning the decay to the lightest Higgs boson  $h_1$ , a correlation is visible. The points explaining both excesses within the  $1\sigma$  uncertainty have larger branching fractions. In order for this decay to happen,  $h_1$  needs a sizable doublet component, otherwise it would not couple to the  $W$  boson. The doublet component is, as explained before, also necessary for  $h_1$  to contribute to the signal strengths at LEP and CMS.

The prospects for the searches for the heavy neutral Higgs bosons, decaying dominantly to  $t\bar{t}$ , may also be promising. However, we are not aware of corresponding HL-LHC projections.

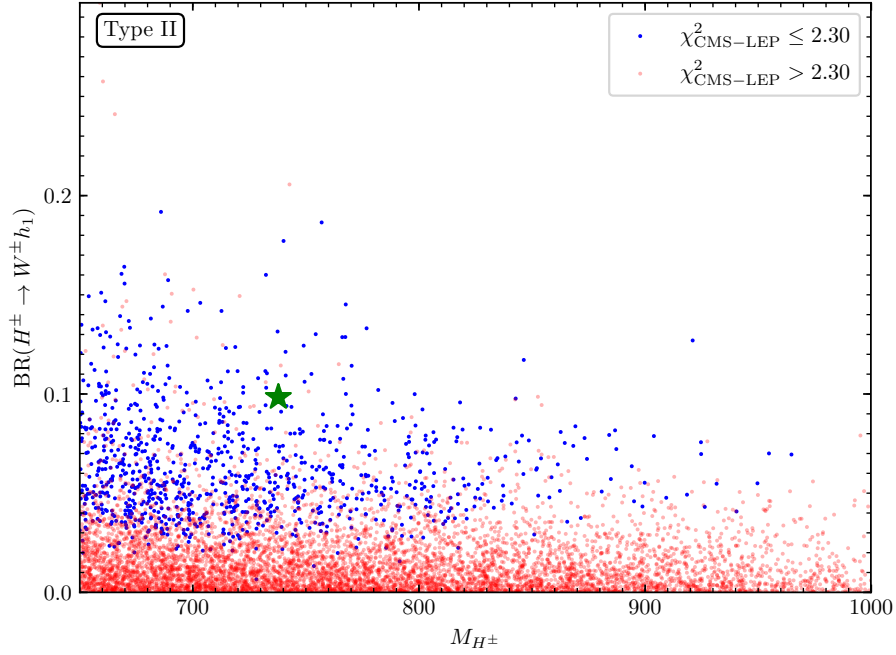


**Figure 4:** Type II: The branching ratios  $BR(H^\pm \rightarrow W^\pm h_1)$  are shown for each parameter point inside (*blue*) and outside (*red*) the  $1\sigma$  ellipse regarding the CMS and the LEP excesses. The best-fit point is marked by the green star.

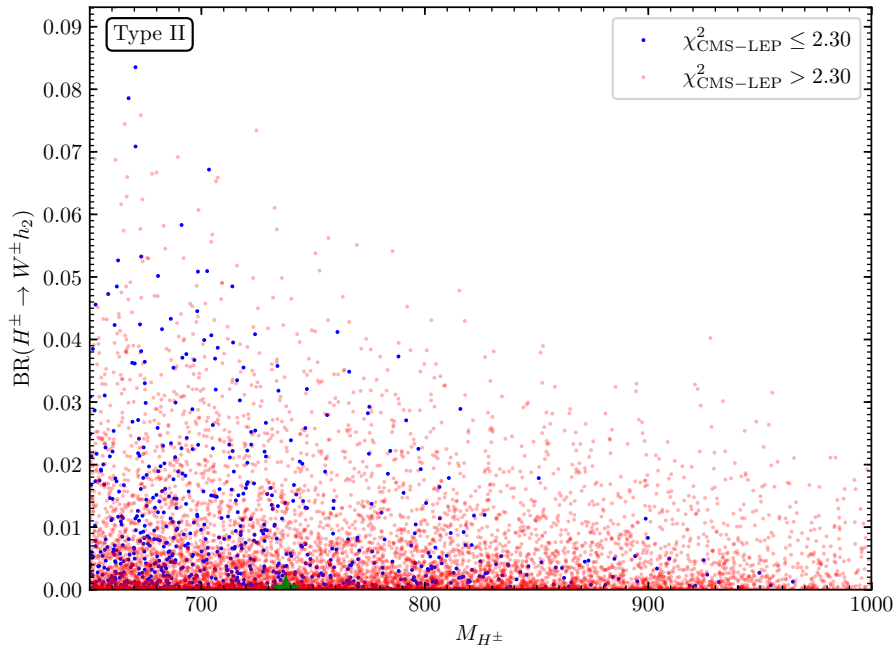


**Figure 5:** Type II: Same as in Fig. 4 for  $BR(H^\pm \rightarrow W^\pm h_2)$ .

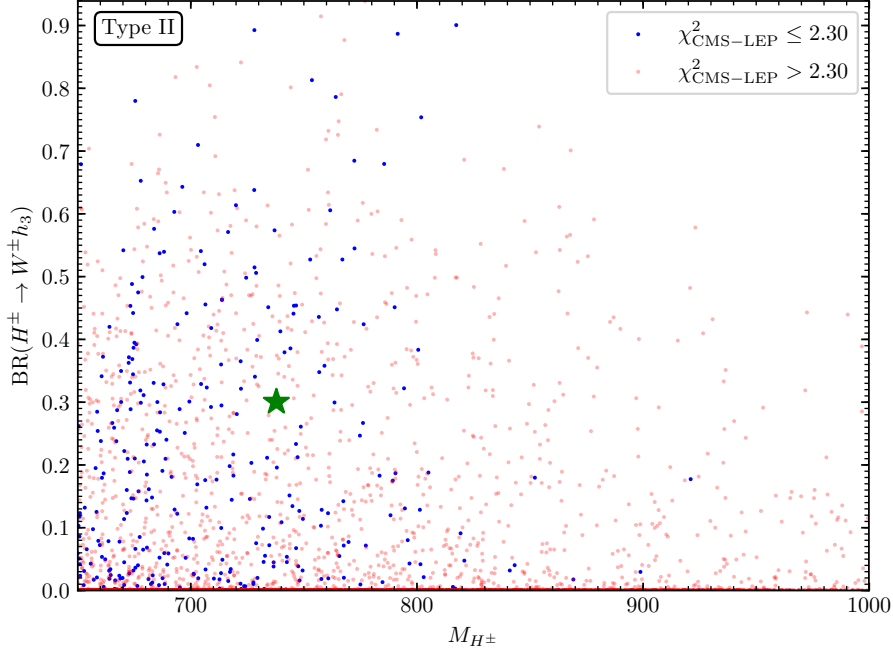


**Figure 6:** Type II: Same as in Fig. 4 for  $\text{BR}(H^\pm \rightarrow W^\pm h_3)$ .

$e^+e^-$  colliders, on the other hand show good prospects for the search of light scalars [50, 60]. The main production channel in the mass and energy range that we are interested in is the Higgsstrahlung process  $e^+e^- \rightarrow \phi Z$ , where  $\phi$  is the scalar being searched for. The LEP collaboration has previously performed such searches [4], which resulted in the  $2\sigma$  excess given by  $\mu_{\text{LEP}}$ . These searches were limited by the low luminosity of LEP. However, the ILC, with its much higher luminosity and the possibility of using polarized beams, has a substantially higher potential to discover the light scalars. The searches performed at LEP can be divided into two categories: the 'traditional method', where studies are based on the decay mode  $\phi \rightarrow b\bar{b}$  along with  $Z$  decays to  $\mu^+\mu^-$  final states. This method introduces certain amount of model dependence into the analysis because of the reference to a specific decay mode of  $\phi$ . The more model independent 'recoil technique' used by the OPAL collaboration of LEP looked for light states by analyzing the recoil mass distribution of the di-muon system produced in  $Z$  decay [61].

In Fig. 7 [23] the bounds from the LEP as well as the projected bounds from the ILC searches for light scalars in type II N2HDM scenarios are shown. The lines indicating the ILC reach for a  $\sqrt{s} = 250$  GeV machine with beam polarizations  $(P_{e^-}, P_{e^+})$  of  $(-80\%, +30\%)$  and an integrated luminosity of  $2000 \text{ fb}^{-1}$  are as evaluated in Ref. [50]. The quantity  $S_{95}$  used in their analysis corresponds to an upper limit at the 95% confidence level on the cross section times branching ratio generated within the 'background only' hypothesis, where the cross section has been normalized to the reference SM-Higgs cross section and the BRs have been assumed to be as in the SM (with a Higgs boson of the same mass). Consequently, we take the obtained limits to be valid for the total cross section times branching ratio. The colored points shown in Fig. 7 are the points of the scans in the type II scenario satisfying all the theoretical and experimental constraints. The plot show that

the parameter points of the scans can completely be covered by searches at the ILC for additional Higgs-like scalars. Depending on  $c_{h_1VV}$ , i.e., the light Higgs-boson production cross section, the  $h_1$  can be produced and analyzed in detail at the ILC.

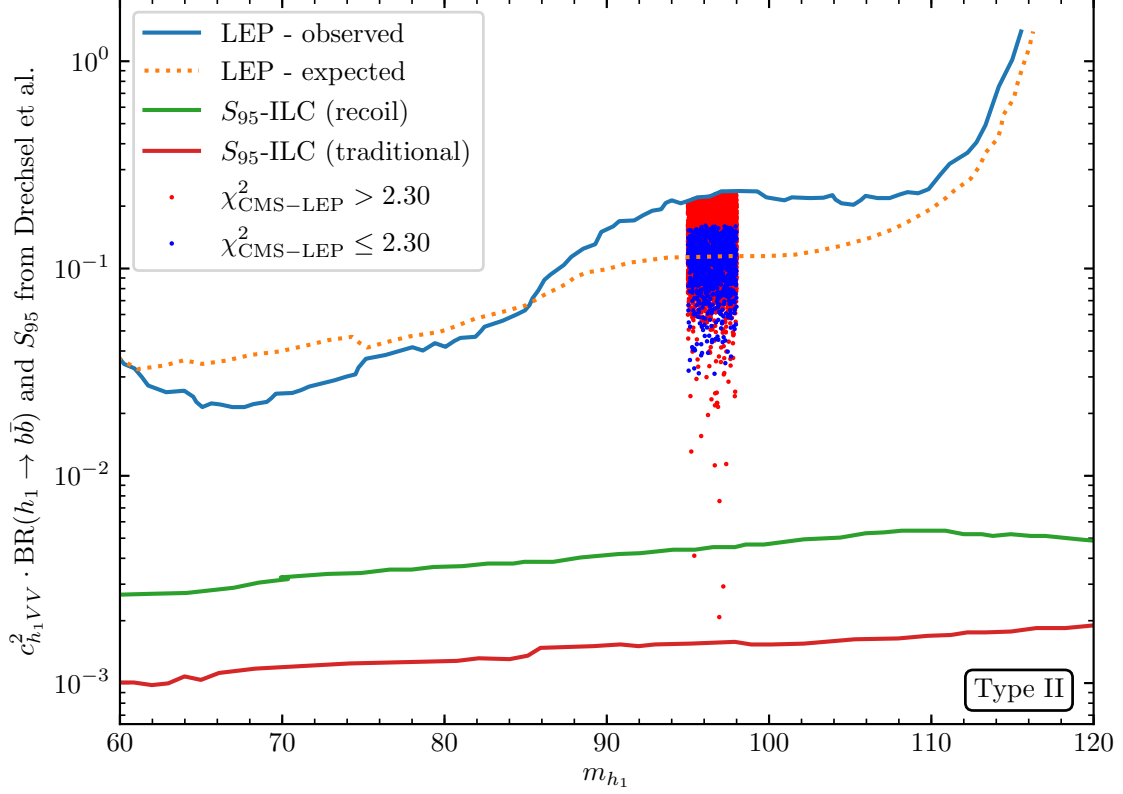


**Figure 7:** The 95% CL expected (*orange dashed*) and observed (*blue*) upper bounds on the Higgsstrahlung production process with associated decay of the scalar to a pair of bottom quarks at LEP [4]. Expected 95% CL upper limits on the Higgsstrahlung production process normalized to the SM prediction  $S_{95}$  at the ILC using the traditional (*red*) and the recoil technique (*green*) as described in the text [50]. We also show the points of our scan in the type II scenario which lie within (*blue*) and outside (*red*) the  $1\sigma$  ellipse regarding the CMS and the LEP excesses.

## 5. Supersymmetric realizations

In Sect. 2.3 it was demonstrated that due to the structure of the couplings of the Higgs doublets to fermions only two types of the N2HDM, type II and type IV (flipped), can fit simultaneously the two excesses. Due to the different coupling to leptons in type II and type IV, in general larger values of  $\mu_{\text{CMS}}$  can be reached in the former, and the CMS excess can be fitted “more naturally” in the type II N2HDM. Incidentally, this is exactly the Higgs sector that is required by supersymmetric models. On the other hand, in Ref. [21] it was shown that the MSSM cannot explain the CMS excess in the diphoton final state. This can be traced back to the “too rigid” structure of the 2HDM (type II) structure of the Higgs-boson sector in the MSSM. SUSY models that can poten-

tially explain both excesses simultaneously, consequently, should contain (at least) an additional Higgs singlet.

Going beyond the MSSM, a well-motivated extension is given by the Next-to-MSSM (NMSSM), see [62, 63] for reviews. In the NMSSM a new singlet superfield is introduced, which only couples to the Higgs- and sfermion-sectors, giving rise to an effective  $\mu$ -term. In the  $\mathcal{C}\mathcal{P}$ -conserving case the NMSSM Higgs sector consists of three  $\mathcal{C}\mathcal{P}$ -even Higgs bosons,  $h_i$  ( $i = 1, 2, 3$ ), two  $\mathcal{C}\mathcal{P}$ -odd Higgs bosons,  $a_j$  ( $j = 1, 2$ ), and the charged Higgs boson pair  $H^\pm$ . In the NMSSM not only the lightest but also the second lightest  $\mathcal{C}\mathcal{P}$ -even Higgs boson can be interpreted as the signal observed at about 125 GeV, see, e.g., [64, 65]. In Ref. [16] it was demonstrated that the NMSSM can indeed simultaneously satisfy the two excesses mentioned above. In this case, the Higgs boson at  $\sim 96$  GeV has a large singlet component, but also a sufficiently large doublet component to give rise to the two excesses.

A natural extension of the NMSSM is the  $\mu\nu$ SJM, in which the singlet superfield is interpreted as a right-handed neutrino superfield [66, 67], see Refs. [68–70] for reviews. The  $\mu\nu$ SJM is the simplest extension of the MSSM that can provide massive neutrinos through a see-saw mechanism at the electroweak scale. A Yukawa coupling for right-handed neutrinos of the order of the electron Yukawa coupling is introduced that induces the explicit breaking of  $R$ -parity. Also in the  $\mu\nu$ SJM the signal at  $\sim 125$  GeV can be interpreted as the lightest or the second lightest  $\mathcal{C}\mathcal{P}$ -even scalar. In Ref. [15] the “one generation case” (only one generation of massive neutrinos) was analyzed. In this case Higgs-boson sector of the  $\mu\nu$ SJM effectively resembles the Higgs-boson sector in the NMSSM. In Ref. [15] it was found that also the  $\mu\nu$ SJM can fit the CMS and the LEP excesses simultaneously. In this case the scalar at  $\sim 96$  GeV has a large right-handed sneutrino component. The three generation case (i.e. with three generations of massive neutrinos) is currently under investigation [71].

## 6. Conclusions

A  $\sim 3\sigma$  excess (local) in the diphoton decay mode at  $\sim 96$  GeV was reported by CMS, as well as a  $\sim 2\sigma$  excess (local) in the  $b\bar{b}$  final state at LEP in the same mass range. We reviewed the interpretation this possible signal as a Higgs boson in the 2 Higgs Doublet Model with an additional real Higgs singlet (N2HDM) [23].

All relevant constraints were included in the analysis. These are theoretical constraints from perturbativity and the requirement that the minimum of the Higgs potential is a global minimum. We take into account the direct searches for additional Higgs bosons from LEP, the Tevatron and the LHC, as well as the measurements of the properties of the Higgs boson at  $\sim 125$  GeV. We furthermore include bounds from flavor physics and from electroweak precision data.

It was demonstrated that due to the structure of the couplings of the Higgs doublets to fermions only two types of the N2HDM, type II and type IV (flipped), can fit simultaneously the two excesses. On the other hand, the other two types, type I and type III (lepton specific), cannot be brought in agreement with the two excesses. Subsequently, the free parameters in the two favored versions of the N2HDM were scanned, where the results are similar in both scenarios. It was found that the lowest possible values of  $M_{H^\pm}$  above  $\sim 650$  GeV and  $\tan\beta$  just above 1 are favored. The reduced  $\chi^2$  from the Higgs-boson measurements is found roughly in the range  $0.9 \lesssim \chi_{\text{red}}^2 \lesssim 1.3$ .

Due to the different coupling to leptons in type II and type IV, in general larger values of  $\mu_{\text{CMS}}$  can be reached in the former, and the CMS excess can be fitted “more naturally” in the type II N2HDM. Incidentally, this is exactly the Higgs sector that is required by supersymmetric models.

It was analyzed how the favored scenarios can be tested at future colliders. The (HL-)LHC will continue the searches/measurements in the diphoton final state. But apart from that we are not aware of other channels for the light Higgs boson that could be accessible. Concerning the searches for heavy N2HDM Higgs bosons, particularly interesting are the prospects for charged Higgs bosons. For the low  $\tan\beta$  values favored in our analysis, these searches have the best potential to discover a new heavy Higgs boson at the LHC Run III or the HL-LHC. The prospects for the searches for the heavy neutral Higgs bosons, decaying dominantly to  $t\bar{t}$ , may also be promising. However, we are not aware of corresponding HL-LHC projections.

A future  $e^+e^-$  collider, such as the ILC, CLIC, FCC-ee or CepC, will be able to produce the light Higgs state at  $\sim 96$  GeV in large numbers and consequently study its decay patterns. Similarly, it was demonstrated that the high anticipated precision in the coupling measurements of the 125 GeV Higgs boson at the ILC, CLIC, FCC-ee, or CepC will allow to find deviations w.r.t. the SM values if the N2HDM with a  $\sim 96$  GeV Higgs boson is realized in nature. Here the coupling of the SM-like Higgs boson to the massive SM gauge bosons appears to be particularly promising.

Based on the fact that type II can fit the two excesses “most naturally”, we reviewed briefly two SUSY solutions to the two excesses: these are models with two Higgs doublets and (effectively) one Higgs singlet: the NMSSM and the (one-generation case)  $\mu\nu\text{SSM}$ . In both models, despite the additional SUSY constraints on the Higgs-boson sector, the two excesses can indeed be fitted simultaneously.

## Acknowledgements

S.H. thanks the organizers of the Corfu Summer Institute 2018 “School and Workshops on Elementary Particle Physics and Gravity” (CORFU2018) for the warm hospitality, the inspiring atmosphere and the excellent “local specialities”.

We thank R. Santos, T. Stefaniak and G. Weiglein for helpful discussions. M.C. thanks D. Azevedo for discussions regarding `ScannerS`. The work was supported in part by the MEINCOP (Spain) under contract FPA2016-78022-P and in part by the AEI through the grant IFT Centro de Excelencia Severo Ochoa SEV-2016-0597. The work of T.B. and S.H. was supported in part by the Spanish Agencia Estatal de Investigación (AEI), in part by the EU Fondo Europeo de Desarrollo Regional (FEDER) through the project FPA2016-78645-P, in part by the “Spanish Red Consolider MultiDark” FPA2017-90566-REDC. The work of T.B. was funded by Fundación La Caixa under ‘La Caixa-Severo Ochoa’ international predoctoral grant.

## References

- [1] **ATLAS** Collaboration, G. Aad *et al.*, “Observation of a new particle in the search for the Standard Model Higgs boson with the ATLAS detector at the LHC”, *Phys. Lett.* **B716** (2012) 1–29, [arXiv:1207.7214](https://arxiv.org/abs/1207.7214).

- [2] CMS Collaboration, S. Chatrchyan *et al.*, “Observation of a new boson at a mass of 125 GeV with the CMS experiment at the LHC”, *Phys. Lett.* **B716** (2012) 30–61, [arXiv:1207.7235](#).
- [3] ATLAS, CMS Collaboration, G. Aad *et al.*, “Measurements of the Higgs boson production and decay rates and constraints on its couplings from a combined ATLAS and CMS analysis of the LHC pp collision data at  $\sqrt{s} = 7$  and 8 TeV”, *JHEP* **08** (2016) 045, [arXiv:1606.02266](#).
- [4] LEP Working Group for Higgs boson searches, ALEPH, DELPHI, L3, OPAL Collaboration, R. Barate *et al.*, “Search for the standard model Higgs boson at LEP”, *Phys. Lett.* **B565** (2003) 61–75, [arXiv:hep-ex/0306033](#).
- [5] J. Cao, X. Guo, Y. He, P. Wu, and Y. Zhang, “Diphoton signal of the light Higgs boson in natural NMSSM”, *Phys. Rev.* **D95** (2017), no. 11, 116001, [arXiv:1612.08522](#).
- [6] A. Azatov, R. Contino, and J. Galloway, “Model-Independent Bounds on a Light Higgs”, *JHEP* **04** (2012) 127, [arXiv:1202.3415](#), [Erratum: *JHEP*04,140(2013)].
- [7] CMS Collaboration, A. M. Sirunyan *et al.*, “Search for a standard model-like Higgs boson in the mass range between 70 and 110 GeV in the diphoton final state in proton-proton collisions at  $\sqrt{s} = 8$  and 13 TeV”, *Submitted to: Phys. Lett.*, 2018 [arXiv:1811.08459](#).
- [8] CMS Collaboration, “Search for new resonances in the diphoton final state in the mass range between 80 and 115 GeV in pp collisions at  $\sqrt{s} = 8$  TeV”, CMS-PAS-HIG-14-037, 2015.
- [9] S. Heinemeyer and T. Stefaniak, “A Higgs Boson at 96 GeV?!”, *PoS CHARGED2018* (2019) 016, [arXiv:1812.05864](#).
- [10] S. Heinemeyer, “A Higgs boson below 125 GeV?!”, *Int. J. Mod. Phys.* **A33** (2018), no. 31, 1844006.
- [11] P. J. Fox and N. Weiner, “Light Signals from a Lighter Higgs”, *JHEP* **08** (2018) 025, [arXiv:1710.07649](#).
- [12] U. Haisch and A. Malinauskas, “Let there be light from a second light Higgs doublet”, *JHEP* **03** (2018) 135, [arXiv:1712.06599](#).
- [13] F. Richard, “Search for a light radion at HL-LHC and ILC250”, [arXiv:1712.06410](#).
- [14] L. Liu, H. Qiao, K. Wang, and J. Zhu, “A light scalar in the Minimal Dilaton Model in light of the LHC constraints”, *Chin. Phys.* **C43** (2019), no. 2, 023104.
- [15] T. Biekotter, S. Heinemeyer, and C. Munoz, “Precise prediction for the Higgs-boson masses in the  $\mu$ VSSM”, *Eur. Phys. J.* **C78** (2018), no. 6, 504, [arXiv:1712.07475](#).
- [16] F. Domingo, S. Heinemeyer, S. PaÅšehr, and G. Weiglein, “Decays of the neutral Higgs bosons into SM fermions and gauge bosons in the  $\mathcal{C}$   $\mathcal{P}$ -violating NMSSM”, *Eur. Phys. J.* **C78** (2018), no. 11, 942, [arXiv:1807.06322](#).

- [17] W. G. Hollik, S. Liebler, G. Moortgat-Pick, S. Pařehř, and G. Weiglein, “Phenomenology of the inflation-inspired NMSSM at the electroweak scale”, *Eur. Phys. J.* **C79** (2019), no. 1, 75, [arXiv:1809.07371](#).
- [18] H. P. Nilles, “Supersymmetry, Supergravity and Particle Physics”, *Phys. Rept.* **110** (1984) 1–162.
- [19] H. E. Haber and G. L. Kane, “The Search for Supersymmetry: Probing Physics Beyond the Standard Model”, *Phys. Rept.* **117** (1985) 75–263.
- [20] S. Heinemeyer, O. Stål, and G. Weiglein, “Interpreting the LHC Higgs Search Results in the MSSM”, *Phys. Lett.* **B710** (2012) 201–206, [arXiv:1112.3026](#).
- [21] P. Bechtle, H. E. Haber, S. Heinemeyer, O. StÅěl, T. Stefaniak, G. Weiglein, and L. Zeune, “The Light and Heavy Higgs Interpretation of the MSSM”, *Eur. Phys. J.* **C77** (2017), no. 2, 67, [arXiv:1608.00638](#).
- [22] H. Bahl, E. Fuchs, T. Hahn, S. Heinemeyer, S. Liebler, S. Patel, P. Slavich, T. Stefaniak, C. E. M. Wagner, and G. Weiglein, “MSSM Higgs Boson Searches at the LHC: Benchmark Scenarios for Run 2 and Beyond”, [arXiv:1808.07542](#).
- [23] T. Biekotter, M. Chakraborti, and S. Heinemeyer, “A 96 GeV Higgs Boson in the N2HDM”, [arXiv:1903.11661](#).
- [24] C.-Y. Chen, M. Freid, and M. Sher, “Next-to-minimal two Higgs doublet model”, *Phys. Rev.* **D89** (2014), no. 7, 075009, [arXiv:1312.3949](#).
- [25] M. Muhlleitner, M. O. P. Sampaio, R. Santos, and J. Wittbrodt, “The N2HDM under Theoretical and Experimental Scrutiny”, *JHEP* **03** (2017) 094, [arXiv:1612.01309](#).
- [26] R. Coimbra, M. O. P. Sampaio, and R. Santos, “ScannerS: Constraining the phase diagram of a complex scalar singlet at the LHC”, *Eur. Phys. J.* **C73** (2013) 2428, [arXiv:1301.2599](#).
- [27] P. Bechtle, O. Brein, S. Heinemeyer, G. Weiglein, and K. E. Williams, “HiggsBounds: Confronting Arbitrary Higgs Sectors with Exclusion Bounds from LEP and the Tevatron”, *Comput. Phys. Commun.* **181** (2010) 138–167, [arXiv:0811.4169](#).
- [28] P. Bechtle, O. Brein, S. Heinemeyer, G. Weiglein, and K. E. Williams, “HiggsBounds 2.0.0: Confronting Neutral and Charged Higgs Sector Predictions with Exclusion Bounds from LEP and the Tevatron”, *Comput. Phys. Commun.* **182** (2011) 2605–2631, [arXiv:1102.1898](#).
- [29] P. Bechtle, O. Brein, S. Heinemeyer, O. StÅěl, T. Stefaniak, G. Weiglein, and K. Williams, “Recent Developments in HiggsBounds and a Preview of HiggsSignals”, *PoS CHARGED2012* (2012) 024, [arXiv:1301.2345](#).
- [30] P. Bechtle, O. Brein, S. Heinemeyer, O. StÅěl, T. Stefaniak, G. Weiglein, and K. E. Williams, “HiggsBounds – 4: Improved Tests of Extended Higgs Sectors against Exclusion

- Bounds from LEP, the Tevatron and the LHC”, *Eur. Phys. J.* **C74** (2014), no. 3, 2693, [arXiv:1311.0055](#).
- [31] P. Bechtle, S. Heinemeyer, O. StÄel, T. Stefaniak, and G. Weiglein, “Applying Exclusion Likelihoods from LHC Searches to Extended Higgs Sectors”, *Eur. Phys. J.* **C75** (2015), no. 9, 421, [arXiv:1507.06706](#).
- [32] P. Bechtle, S. Heinemeyer, O. StÄel, T. Stefaniak, and G. Weiglein, “*HiggsSignals*: Confronting arbitrary Higgs sectors with measurements at the Tevatron and the LHC”, *Eur. Phys. J.* **C74** (2014), no. 2, 2711, [arXiv:1305.1933](#).
- [33] O. StÄel and T. Stefaniak, “Constraining extended Higgs sectors with *HiggsSignals*”, *PoS EPS-HEP2013* (2013) 314, [arXiv:1310.4039](#).
- [34] P. Bechtle, S. Heinemeyer, O. StÄel, T. Stefaniak, and G. Weiglein, “Probing the Standard Model with Higgs signal rates from the Tevatron, the LHC and a future ILC”, *JHEP* **11** (2014) 039, [arXiv:1403.1582](#).
- [35] R. V. Harlander, S. Liebler, and H. Mantler, “SusHi: A program for the calculation of Higgs production in gluon fusion and bottom-quark annihilation in the Standard Model and the MSSM”, *Comput. Phys. Commun.* **184** (2013) 1605–1617, [arXiv:1212.3249](#).
- [36] R. V. Harlander, S. Liebler, and H. Mantler, “SusHi Bento: Beyond NNLO and the heavy-top limit”, *Comput. Phys. Commun.* **212** (2017) 239–257, [arXiv:1605.03190](#).
- [37] A. Djouadi, J. Kalinowski, and M. Spira, “HDECAY: A Program for Higgs boson decays in the standard model and its supersymmetric extension”, *Comput. Phys. Commun.* **108** (1998) 56–74, [arXiv:hep-ph/9704448](#).
- [38] J. M. Butterworth *et al.*, “THE TOOLS AND MONTE CARLO WORKING GROUP Summary Report from the Les Houches 2009 Workshop on TeV Colliders”, in “Physics at TeV colliders. Proceedings, 6th Workshop, dedicated to Thomas Binoth, Les Houches, France, June 8-26, 2009”. 2010. [arXiv:1003.1643](#).
- [39] A. Arbey, F. Mahmoudi, O. StÄel, and T. Stefaniak, “Status of the Charged Higgs Boson in Two Higgs Doublet Models”, *Eur. Phys. J.* **C78** (2018), no. 3, 182, [arXiv:1706.07414](#).
- [40] M. E. Peskin and T. Takeuchi, “A New constraint on a strongly interacting Higgs sector”, *Phys. Rev. Lett.* **65** (1990) 964–967.
- [41] M. E. Peskin and T. Takeuchi, “Estimation of oblique electroweak corrections”, *Phys. Rev.* **D46** (1992) 381–409.
- [42] **ALEPH, DELPHI, L3, OPAL, LEP Working Group for Higgs Boson Searches** Collaboration, S. Schael *et al.*, “Search for neutral MSSM Higgs bosons at LEP”, *Eur. Phys. J.* **C47** (2006) 547–587, [arXiv:hep-ex/0602042](#).

- [43] S. Gascon-Shotkin, “Update on Higgs searches below 125 GeV”.  
*Higgs Days at Sandander 2017*,  
<https://indico.cern.ch/event/666384/contributions/2723427/>.
- [44] **LHC Higgs Cross Section Working Group** Collaboration, S. Heinemeyer *et al.*,  
“Handbook of LHC Higgs Cross Sections: 3. Higgs Properties”, [arXiv:1307.1347](https://arxiv.org/abs/1307.1347).
- [45] **Physics of the HL-LHC Working Group** Collaboration, M. Cepeda *et al.*, “Higgs Physics at the HL-LHC and HE-LHC”, [arXiv:1902.00134](https://arxiv.org/abs/1902.00134).
- [46] P. Bambade *et al.*, “The International Linear Collider: A Global Project”,  
[arXiv:1903.01629](https://arxiv.org/abs/1903.01629).
- [47] **CMS** Collaboration, A. M. Sirunyan *et al.*, “Combined measurements of Higgs boson couplings in proton-proton collisions at  $\sqrt{s} = 13$  TeV”, *Submitted to: Eur. Phys. J.*, 2018  
[arXiv:1809.10733](https://arxiv.org/abs/1809.10733).
- [48] **ATLAS** Collaboration, “Combined measurements of Higgs boson production and decay using up to 80 fb<sup>-1</sup> of proton-proton collision data at  $\sqrt{s} = 13$  TeV collected with the ATLAS experiment”, ATLAS-CONF-2018-031, Jul 2018.
- [49] S. Dawson *et al.*, “Working Group Report: Higgs Boson”, in “Proceedings, 2013 Community Summer Study on the Future of U.S. Particle Physics: Snowmass on the Mississippi (CSS2013): Minneapolis, MN, USA, July 29-August 6, 2013”. 2013.  
[arXiv:1310.8361](https://arxiv.org/abs/1310.8361).
- [50] P. Drechsel, G. Moortgat-Pick, and G. Weiglein, “Sensitivity of the ILC to light Higgs masses”, in “International Workshop on Future Linear Collider (LCWS2017) Strasbourg, France, October 23-27, 2017”. 2018. [arXiv:1801.09662](https://arxiv.org/abs/1801.09662).
- [51] **CMS** Collaboration, “Projected Performance of an Upgraded CMS Detector at the LHC and HL-LHC: Contribution to the Snowmass Process”, in “Proceedings, 2013 Community Summer Study on the Future of U.S. Particle Physics: Snowmass on the Mississippi (CSS2013): Minneapolis, MN, USA, July 29-August 6, 2013”. 2013.  
[arXiv:1307.7135](https://arxiv.org/abs/1307.7135).
- [52] **CMS, ATLAS** Collaboration, A. Tricomi, “Prospects of the high luminosity LHC from ATLAS and CMS”, *PoS EPS-HEP2015* (2015) 121.
- [53] **ATLAS** Collaboration, “Projections for measurements of Higgs boson signal strengths and coupling parameters with the ATLAS detector at a HL-LHC”, ATLAS-PHYS-PUB-2014-016, Oct 2014.
- [54] M. Slawinska, “High-luminosity LHC prospects with the upgraded ATLAS detector”, *PoS DIS2016* (2016) 266, [arXiv:1609.08434](https://arxiv.org/abs/1609.08434).
- [55] D. M. Asner *et al.*, “ILC Higgs White Paper”, in “Proceedings, 2013 Community Summer Study on the Future of U.S. Particle Physics: Snowmass on the Mississippi (CSS2013): Minneapolis, MN, USA, July 29-August 6, 2013”. 2013. [arXiv:1310.0763](https://arxiv.org/abs/1310.0763).

- [56] H. Ono and A. Miyamoto, “A study of measurement precision of the Higgs boson branching ratios at the International Linear Collider”, *Eur. Phys. J.* **C73** (2013), no. 3, 2343, [arXiv:1207.0300](#).
- [57] C. D’Aijrig, K. Fujii, J. List, and J. Tian, “Model Independent Determination of  $HWW$  coupling and Higgs total width at ILC”, in “International Workshop on Future Linear Colliders (LCWS13) Tokyo, Japan, November 11-15, 2013”. 2014. [arXiv:1403.7734](#).
- [58] K. Fujii *et al.*, “Physics Case for the 250 GeV Stage of the International Linear Collider”, [arXiv:1710.07621](#).
- [59] M. Guchait and A. H. Vijay, “Probing Heavy Charged Higgs Boson at the LHC”, *Phys. Rev.* **D98** (2018), no. 11, 115028, [arXiv:1806.01317](#).
- [60] Y. Wang, J. List, and M. Berggren, “Search for Light Scalars Produced in Association with Muon Pairs for  $\sqrt{s} = 250$  GeV at the ILC”, in “International Workshop on Future Linear Collider (LCWS2017) Strasbourg, France, October 23-27, 2017”. 2018. [arXiv:1801.08164](#).
- [61] **OPAL** Collaboration, G. Abbiendi *et al.*, “Decay mode independent searches for new scalar bosons with the OPAL detector at LEP”, *Eur. Phys. J.* **C27** (2003) 311–329, [arXiv:hep-ex/0206022](#).
- [62] U. Ellwanger, C. Hugonie, and A. M. Teixeira, “The Next-to-Minimal Supersymmetric Standard Model”, *Phys. Rept.* **496** (2010) 1–77, [arXiv:0910.1785](#).
- [63] M. Maniatis, “The Next-to-Minimal Supersymmetric extension of the Standard Model reviewed”, *Int. J. Mod. Phys.* **A25** (2010) 3505–3602, [arXiv:0906.0777](#).
- [64] S. F. King, M. Muhlleitner, and R. Nevzorov, “NMSSM Higgs Benchmarks Near 125 GeV”, *Nucl. Phys.* **B860** (2012) 207–244, [arXiv:1201.2671](#).
- [65] F. Domingo and G. Weiglein, “NMSSM interpretations of the observed Higgs signal”, *JHEP* **04** (2016) 095, [arXiv:1509.07283](#).
- [66] D. E. Lopez-Fogliani and C. Munoz, “Proposal for a Supersymmetric Standard Model”, *Phys. Rev. Lett.* **97** (2006) 041801, [arXiv:hep-ph/0508297](#).
- [67] N. Escudero, D. E. Lopez-Fogliani, C. Munoz, and R. Ruiz de Austri, “Analysis of the parameter space and spectrum of the mu nu SSM”, *JHEP* **12** (2008) 099, [arXiv:0810.1507](#).
- [68] C. Munoz, “Phenomenology of a New Supersymmetric Standard Model: The mu nu SSM”, *AIP Conf. Proc.* **1200** (2010), no. 1, 413–416, [arXiv:0909.5140](#).
- [69] C. Muñoz, “Searching for SUSY and decaying gravitino dark matter at the LHC and Fermi-LAT with the  $\mu\nu$ SSM”, *PoS DSU2015* (2016) 034, [arXiv:1608.07912](#).

- [70] P. Ghosh, I. Lara, D. E. Lopez-Fogliani, C. Munoz, and R. Ruiz de Austri, “Searching for left sneutrino LSP at the LHC”, *Int. J. Mod. Phys. A* **33** (2018), no. 18n19, 1850110, [arXiv:1707.02471](https://arxiv.org/abs/1707.02471).
- [71] T. Biekotter, S. Heinemeyer, and C. Munoz, “Precise prediction for the Higgs-boson masses in the full  $\mu\nu$ S $SM$ ”, IFT–UAM–CSIC–19-030.